

Technical Report  
842

# Moment Method Analysis of Near-Field Adaptive Nulling

A.J. Fenn

7 April 1989

---

**Lincoln Laboratory**

MASSACHUSETTS INSTITUTE OF TECHNOLOGY

*LExINGTON, MASSACHUSETTS*



---

Prepared for the Department of the Army  
under Electronic Systems Division Contract F19628-85-C-0002.

Approved for public release; distribution is unlimited.

ADA208228

The work reported in this document was performed at Lincoln Laboratory, a center for research operated by Massachusetts Institute of Technology, with the support of the Department of the Army under Air Force Contract F19628-85-C-0002.

This report may be reproduced to satisfy needs of U.S. Government agencies.

The views and conclusions contained in this document are those of the contractor and should not be interpreted as necessarily representing the official policies, either expressed or implied, of the United States Government.

The ESD Public Affairs Office has reviewed this report, and it is releasable to the National Technical Information Service, where it will be available to the general public, including foreign nationals.

This technical report has been reviewed and is approved for publication.

FOR THE COMMANDER

*Hugh L. Southall*

Hugh L. Southall, Lt. Col., USAF  
Chief, ESD Lincoln Laboratory Project Office

Non-Lincoln Recipients

**PLEASE DO NOT RETURN**

Permission is given to destroy this document  
when it is no longer needed.

MASSACHUSETTS INSTITUTE OF TECHNOLOGY  
LINCOLN LABORATORY

**MOMENT METHOD ANALYSIS OF  
NEAR-FIELD ADAPTIVE NULLING**

*A.J. FENN*  
*Group 61*

TECHNICAL REPORT 842

7 APRIL 1989

Approved for public release; distribution is unlimited.

LEXINGTON

MASSACHUSETTS

## ACKNOWLEDGMENTS

I wish to express my gratitude to J.R. Johnson for technical discussions.

## ABSTRACT

A near-field technique which can be used to evaluate the far-field nulling characteristics of an adaptive phased array is investigated. The method of moments is used to analyze the performance of a side-lobe canceller adaptive phased array antenna operating in the presence of near-field interference. Bandwidth, polarization, mutual coupling, and finite array edge effects are taken into account. Phased array near-field focusing is used to produce an equivalent far-field antenna pattern at a range distance of one to two aperture diameters from the adaptive antenna under test. It is shown that the near-field adaptive nulling performance, with sources located on a test plane at *one- to two-aperture-diameters range*, is equivalent to conventional far-field adaptive nulling. The antenna analyzed is a planar array of monopole elements having multiple auxiliary channels. The interferer is assumed to be a band-limited noise source radiating from a dipole antenna. The adaptive nulling characteristics studied in detail are the array radiation patterns, adaptive cancellation, covariance matrix eigenvalues (degrees of freedom), and adaptive array weights.

## TABLE OF CONTENTS

ACKNOWLEDGMENTS	iii
ABSTRACT	v
LIST OF ILLUSTRATIONS	ix
1. INTRODUCTION	1
2. THEORY	3
2.1 Focused Near-Field Nulling Concept	3
2.2 Adaptive Array Concepts	3
2.3 Moment Method Formulation	6
3. RESULTS	11
3.1 Focused Array Quiescent Conditions	11
3.2 Sidelobe Canceller Adaptive Array Behavior	12
4. CONCLUSION	21
REFERENCES	23
APPENDIX A – DERIVATION OF ARRAY RECEIVED VOLTAGE MATRIX	25

## LIST OF ILLUSTRATIONS

Figure No.		Page
1-1	Contrast Between Plane Wave Incidence (Far-Field Source) and Spherical Wave Incidence (Near-Field Source) for an Adaptive Array Aperture	1
2-1	Adaptive Phased Array Antenna Near-Field Focusing Concept	4
2-2	Circuit Model for Receive Array with Near-Field Source	7
2-3	Example Near-Field Scan Lengths: (a) 60° and (b) 120° Field of View.	9
3-1	Planar Array of Monopoles with Dipole Source	11
3-2	Monopole Array NF/FF Radiation Patterns (One Interferer) Before Nulling: (a) $F/L = 1$ , (b) $F/L = 1.5$ , and (c) $F/L = 2$ .	13
3-3	Monopole Array NF/FF Radiation Patterns After Nulling: (a) $F/L = 1$ , (b) $F/L = 1.5$ , and (c) $F/L = 2$ .	14
3-4	Covariance Matrix Eigenvalues for One NF/FF Interferer	15
3-5	Amplitude of Adaptive Weights for One NF/FF Interferer	16
3-6	Two-Dimensional Near-Field Radiation Pattern After Adaption	16
3-7	Monopole Array NF/FF Radiation Patterns (Two Interferers) After Nulling: (a) $F/L = 1$ , (b) $F/L = 1.5$ , and (c) $F/L = 2$ .	18
3-8	Covariance Matrix Eigenvalues for Two NF/FF Interferers Versus Nulling Bandwidth: (a) $\lambda_1, \lambda_2$ and (b) $\lambda_3, \lambda_4$ .	19
3-9	Adaptive Cancellation for Two NF/FF Interferers Versus Nulling Bandwidth	20
3-10	Amplitude of Adaptive Weights for Two NF/FF Interferers	20

# 1. INTRODUCTION

Phased array antennas having adaptive nulling capability are often desirable for radar or communications applications. The adaptive nulling performance of these antennas is principally tested using conventional far-field antenna ranges with far-field (or plane wave) interferers. For electrically large antennas at microwave frequencies, this can lead to significant far-field range distances which require that testing be made outdoors. Multiple, widely separated interferers make the far-field range design more difficult. Near-field testing, suitable for indoor measurements is desirable (as has been demonstrated in the case of near-field scanning [1]) for far-field pattern measurements and compact range reflector techniques [2] for far-field radiation pattern and radar cross-section measurements. In both the near-field scanning and compact range methods, the goal is to evaluate the plane wave response of a test article.

If the requirement for plane wave test conditions is removed and spherical wave incidence is allowed (as will be shown theoretically) for a focused phased array adaptive antenna, near-field testing with an interferer at *one- to two- aperture-diameters range* is possible. The contrast between plane wave and spherical wave incidence is depicted in Figure 1-1. The amount of wavefront dispersion observed by the array is a function of the bandwidth, array length, and angle of incidence. Interference wavefront dispersion is an effect which can limit the depth of null (or cancellation) achieved by an adaptive antenna [3].

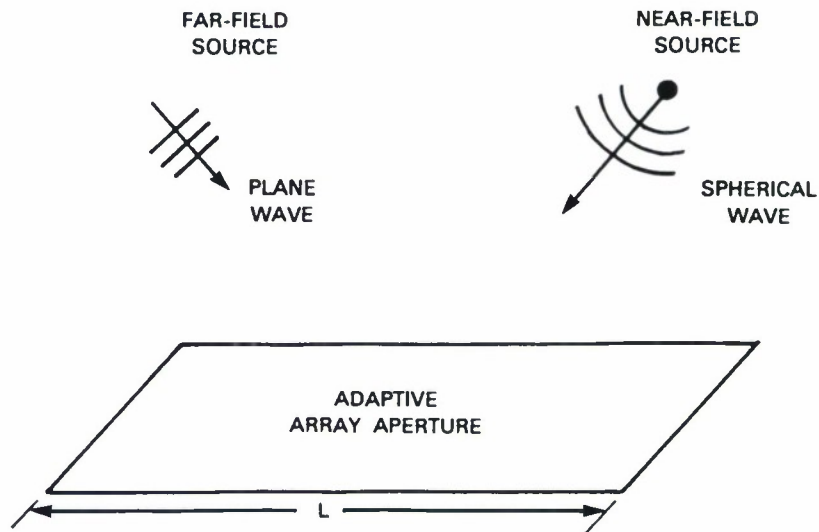


Figure 1-1. Contrast between plane wave incidence (far-field source) and spherical wave incidence (near-field source) for an adaptive array aperture.

115090-1

A precise dispersion model is essentially the characteristics of the interference covariance matrix – namely its eigenvalues or degrees of freedom [3,4]. The covariance matrix contains all wavefront dispersion presented to the adaptive channels. The interference covariance matrix eigenvalues can be used to quantify and to compare the dispersion present for plane wave and spherical wave incidence. For near-field (NF) adaptive nulling to be equivalent to far-field (FF) adaptive nulling, it is assumed that the NF/FF interference covariance matrix eigenvalues must be equivalent. Additionally, it is assumed that the NF/FF adaptive array weights, cancellation of interference power, and radiation patterns must also be equivalent.

Investigations of NF/FF adaptive nulling for focused linear arrays of isotropic receive elements have been performed [5-9]. Near-field adaptive nulling results for a single interferer at a range of  $1.7 L$  for side-lobe canceller [5,6] and fully adaptive [5,7] arrays have been presented. The effects of nulling bandwidth were taken into account. Comparisons with far-field adaptive nulling indicated an excellent NF/FF equivalence. A detailed analysis of near-field nulling for a fully adaptive array with single and multiple interferers, in the range of one to two aperture diameters, has been made [8]. Application of this near-field technique to testing main beam clutter cancellation is also documented [9]. Having shown the usefulness of focused near-field nulling under the conditions of isotropic receive antennas and isotropic interference, it is now appropriate to consider the effects of polarization and mutual coupling. References 5 to 9 assumed that all sources are constrained to be located at a constant range with respect to the phase center of the antenna under test. The present report seeks to have compatibility with planar near-field scanner hardware. Thus, all sources are assumed to be located on a test plane.

A theory for analyzing and comparing both near- and far-field adaptive nulling, including mutual coupling effects, is presented in Chapter 2. Near-field focusing and the near-field nulling concept are described first. General adaptive nulling concepts are then addressed. A method-of-moments formulation for the voltages received by the array elements is then given. The appendix contains a derivation of the array received voltage matrix. Computation of the interference covariance matrix and array radiation patterns is described. Chapter 3 presents results which show that an adaptive array responds in the same manner to near-field as it does to far-field sources.

## 2. THEORY

### 2.1 FOCUSED NEAR-FIELD NULLING CONCEPT

In the near-field nulling technique described here, it is assumed that the quiescent near-field radiation pattern of the array should have the same characteristics as the quiescent far-field radiation pattern of the array. This means typically that a main beam and side lobes should be formed. To produce an array near-field pattern which is approximately equal to that of the far-field, phase focusing can be used [10]. Consider Figure 2-1 which shows a CW calibration source located at a desired focal point of the array. The array can maximize the signal received from the calibration source by adjusting its phase shifters such that the spherical wavefront phase variation is removed. One way to do this is to choose a reference path length as the distance from the focal point to the center of the array. This distance is denoted  $r_F$ , and the distance from the focal point to the  $n$ th array element is denoted  $r_n^F$ . The voltage received at the  $n$ th array element relative to its center element is computed here using the method of moments. To maximize the received voltage at the array output, it is necessary to apply the phase conjugate of the incident wavefront at the array elements. The resulting radiation pattern on the test plane  $z = z_F$  looks similar to a far-field pattern. A main beam will be pointed at the array focal point. Sidelobes will exist at angles away from the main beam. Interferers can then be placed on near-field sidelobes in the test (or focal) plane, as depicted in Figure 2-1.

### 2.2 ADAPTIVE ARRAY CONCEPTS

Consider the array and interferer geometry as shown in Figure 2-1. In general, the array will contain a total of  $N$  elements, with only  $N_r$  elements used to form the receive main channel. This is often the case with arrays having a guard band of passively terminated elements, which is used to provide impedance matching to the active elements and/or isolation from ground plane edges. The output from each of the  $N_r$  array elements is summed in the power combiner to form the main channel. Let a wavefront (either planar or spherical) due to the  $i$ th interference source, be impressed across the array, which results in a set of array element received voltages denoted  $v_1^i, v_2^i, \dots, v_N^i$ . The number of adaptive channels is denoted  $M$ . For a sidelobe canceller  $M = 1 + N_{\text{aux}}$  where  $N_{\text{aux}}$  is the number of auxiliary channels. The main and auxiliary channel voltages are selected from among the above set of array received voltages. In this report, ideal weights are assumed with  $\mathbf{w} = (w_1, w_2, \dots, w_M)^T$  denoting the adaptive channel weight vector and  $\mathbf{W} = (W_1, W_2, \dots, W_N)^T$  denoting the sidelobe canceller array element weight vector, as shown in Figure 2-1. (Superscript  $T$  means transpose.) The fundamental quantities required to fully characterize the incident field for adaptive nulling purposes are the adaptive channel cross correlations.

The cross correlation  $R_{mn}^i$  of the received voltages in the  $m$ th and  $n$ th adaptive channels, due to the  $i$ th source, is given by

$$R_{mn}^i = \mathbf{E}(v_m v_n^*) \quad (2.1)$$

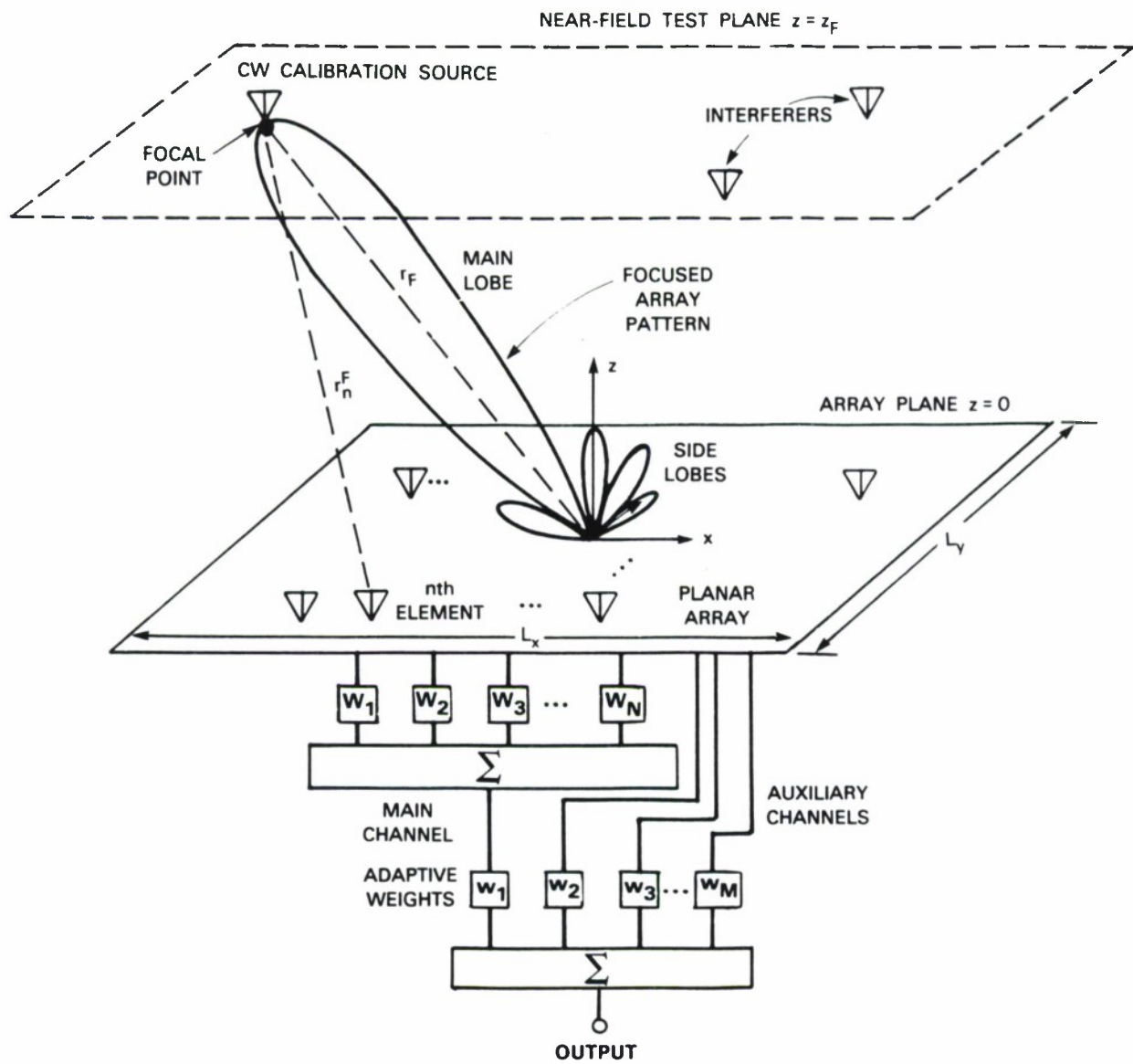


Figure 2-1. Adaptive phased array antenna near-field focusing concept.

where  $*$  means complex conjugate and  $E(\cdot)$  means mathematical expectation. Since  $v_m$  and  $v_n$  represent voltages of the same waveform, but at different times,  $R_{mn}^i$  is also referred to as an autocorrelation function. Note: For convenience, in Equation (2.1) the superscript  $i$  in  $v_m$  and in  $v_n$  has been omitted.

In the frequency domain, assuming the interference has a band-limited white noise power spectral density, Equation (2.1) can be expressed as the frequency average

$$R_{mn}^i = \frac{1}{B} \int_{f_1}^{f_2} v_m(f) v_n^*(f) df \quad (2.2)$$

where  $B = f_2 - f_1$  is the nulling bandwidth and  $f_c$  is the center frequency. It should be noted that  $v_m(f)$  takes into account the wavefront shape which can be spherical or planar.

Let the channel or interference covariance matrix be denoted  $\mathbf{R}$ . If there are  $J$  uncorrelated broadband interference sources, then the  $J$ -source covariance matrix is the sum of the covariance matrices for the individual sources, that is,

$$\mathbf{R} = \sum_{i=1}^J \mathbf{R}_i + \mathbf{I} \quad (2.3)$$

where  $\mathbf{R}_i$  is the covariance matrix of the  $i$ th source,  $\mathbf{I}$  is the identity matrix which is used to represent the thermal noise level of the receiver.

Prior to generating an adaptive null, the adaptive channel weight vector,  $\mathbf{w}$ , is chosen to synthesize a desired quiescent radiation pattern. When interference is present, the optimum set of weights, denoted  $\mathbf{w}_a$ , to form an adaptive null is computed by [11]

$$\mathbf{w}_a = \mathbf{R}^{-1} \mathbf{w}_q \quad (2.4)$$

where  $^{-1}$  means inverse and  $\mathbf{w}_q$  is the quiescent weight vector. For a side-lobe canceller, the quiescent weight vector is chosen to be  $\mathbf{w}_q = (1, 0, 0, \dots, 0)^T$ , that is, the main channel weight is unity and the auxiliary channel weights are zero.

The output power at the adaptive array summing junction is given by

$$p = \mathbf{w}^\dagger \mathbf{R} \mathbf{w} \quad (2.5)$$

where  $^\dagger$  means complex conjugate transpose. The interference-plus-noise-to-noise ratio, denoted  $INR$ , is computed as the ratio of the output power [defined in Equation (2.5)] with the interferer present to the output power with only receiver noise present, that is,

$$INR = \frac{\mathbf{w}^\dagger \mathbf{R} \mathbf{w}}{\mathbf{w}^\dagger \mathbf{w}}. \quad (2.6)$$

The adaptive array cancellation ratio, denoted  $C$ , is defined here as the ratio of interference output power after adaption to the interference output power before adaption, that is,

$$C = \frac{p_a}{p_q}. \quad (2.7)$$

Substituting Equation (2.5) in (2.7) yields

$$C = \frac{\mathbf{w}_a^\dagger \mathbf{R} \mathbf{w}_a}{\mathbf{w}_q^\dagger \mathbf{R} \mathbf{w}_q}. \quad (2.8)$$

Next, the covariance matrix defined by the elements in Equation (2.2) is Hermitian (that is,  $\mathbf{R} = \mathbf{R}^\dagger$ ) which, by the spectral theorem, can be decomposed in eigenspace as [12]

$$\mathbf{R} = \sum_{k=1}^M \lambda_k \mathbf{e}_k \mathbf{e}_k^\dagger \quad (2.9)$$

where  $\lambda_k, k = 1, 2, \dots, M$  are the eigenvalues of  $\mathbf{R}$ , and  $\mathbf{e}_k, k = 1, 2, \dots, M$  are the associated eigenvectors of  $\mathbf{R}$ . The interference covariance matrix eigenvalues ( $\lambda_1, \lambda_2, \dots, \lambda_M$ ) are a convenient quantitative measure of the utilization of the adaptive array degrees of freedom.

### 2.3 MOMENT METHOD FORMULATION

This section considers using the method of moments [13] to compute the array element received voltages in Equation (2.2) due to near- or far-field sources. The far-field formulation given here is analogous to that which has been developed by Gupta [14]. Referring to Figure 2-2, assume that each element is terminated in the load impedance  $Z_L$  which is known. Let  $v_{n,j}^{o.c.}$  represent the open-circuit voltage in the  $n$ th array element due to the  $j$ th source. Here, the  $j$ th source can denote either the CW calibrator or one of the broadband noise interferers. Next, let  $\mathbf{Z}^{o.c.}$  be the open-circuit mutual impedance matrix for the  $N$ -element array. It is shown in Appendix A that the array received voltage matrix, denoted  $\mathbf{v}_j^{\text{rec}}$ , due to the  $j$ th source, can be expressed as

$$\mathbf{v}_j^{\text{rec}} = Z_L [\mathbf{Z}^{o.c.} + Z_L \mathbf{I}]^{-1} \mathbf{v}_j^{o.c.} \quad (2.10)$$

In Equation (2.10), the  $n$ th element of  $\mathbf{v}_j^{o.c.}$  is computed, for near-field sources, using the relation

$$v_{n,j}^{o.c.} = i_j Z_{n,j}^{o.c.} \quad (2.11)$$

where  $i_j$  is the terminal current for the  $j$ th source and  $Z_{n,j}^{o.c.}$  is the open-circuit mutual impedance between the  $j$ th source and the  $n$ th array element. The moment method expansion and testing functions are assumed to be piecewise sinusoidal, which is appropriate to thin cylindrical-wire monopole/dipole antennas. The above open-circuit mutual impedances are computed based on subroutines from a well-known moment method computer code [15]. In evaluating  $Z_{n,j}^{o.c.}$  for the  $j$ th interferer, double precision computations were required. For far-field sources,  $v_{n,j}^{o.c.}$  is evaluated by assuming plane wave incidence.

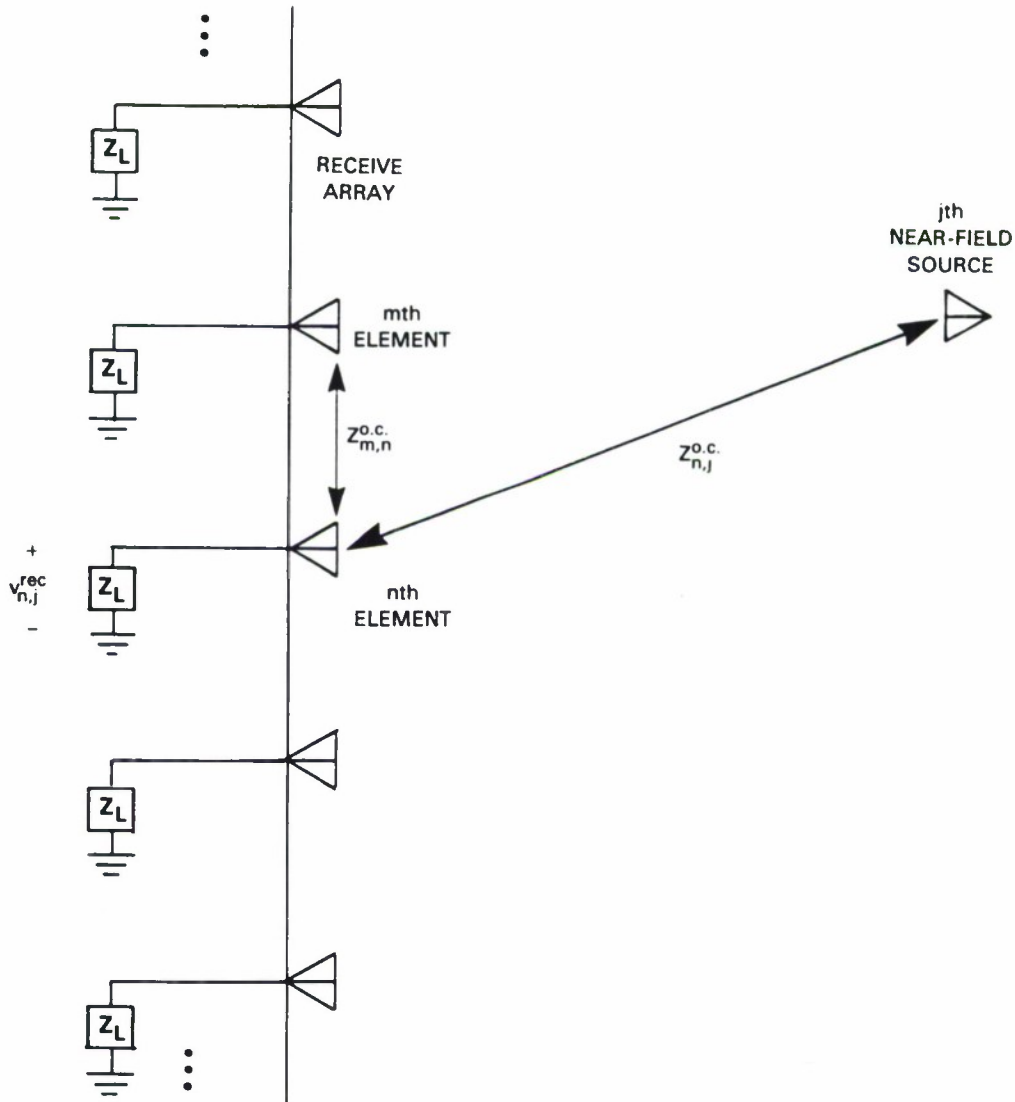


Figure 2-2. Circuit model for receive array with near-field source.

As mentioned earlier, the array is calibrated (phased focused) initially using a CW radiating dipole. To accomplish this numerically, having computed  $v_{CW}^{rec}$ , the receive array weight vector  $\mathbf{W}$  will have its phase commands set equal to the conjugate of the corresponding phases in  $v_{CW}^{rec}$ . Receive antenna radiation patterns are obtained by scanning (moving) a dipole with half-length  $l$  in either the far- or near-field and computing the antenna response. Far-field received patterns are computed using a  $\hat{\theta}$ -polarized dipole source at infinity which generates plane wave illumination of the array. Principal plane near-field radiation pattern cuts (versus angle) are obtained by computing the near field on the line  $(x, y = 0, z = z_F)$  and using the relation  $\theta(x) = \tan^{-1}(x/z_F)$ . The near-field source is a one-half wavelength dipole which is  $\hat{x}$ -polarized. Let the voltage received by the array, due to the  $x$ -directed near-field dipole, be denoted  $v_x^{NF}(\theta)$ . Let  $p_\theta(\theta)$  denote the  $\hat{\theta}$  component of the dipole probe pattern. Then the probe-compensated array near-field received pattern is expressed as

$$E_{\theta}(\theta)^{NF} = \frac{v_x^{NF}(\theta)}{p_{\theta}(\theta)} \quad (2.12)$$

where

$$p_{\theta}(\theta) = \frac{\cos(\beta l \sin \theta) - \cos(\beta l)}{\cos \theta}. \quad (2.13)$$

Equation (2.12) is correct provided that the radial component of the electric field is zero. For the test distances involved in this report, the radial component  $E_r$  is typically -30 dB below the  $E_{\theta}$  component, according to theoretical calculations. Thus, for all practical purposes the equality in Equation (2.12) is valid. (Further discussion of the near-field radial component is deferred to a future report.) Let  $\theta_{\max}$  denote the maximum angle of interest for the antenna radiation pattern. The required near-field scan length for pattern coverage of  $\pm\theta_{\max}$  is given in terms of the  $F/L$  ratio as

$$D_x = 2L\left(\frac{F}{L}\right) \tan \theta_{\max}. \quad (2.14)$$

As an example, Figure 2-3(a,b) depicts the required scan lengths for 60° and 120° field-of-view coverage using  $F/L$  ratios of 1, 1.5, and 2  $L$ . It is clear that to reduce the scan length (or source deployment length) it is desirable to keep the  $F/L$  ratio as small as possible.

The array received voltage matrix for the  $j$ th interferer (denoted  $\mathbf{v}_j^{\text{rec}}$ ) is computed at  $K$  frequencies across the nulling bandwidth. Thus,  $\mathbf{v}_j^{\text{rec}}(f_1), \mathbf{v}_j^{\text{rec}}(f_2), \dots, \mathbf{v}_j^{\text{rec}}(f_K)$  are needed. In this report, the impedance matrix is computed at  $K$  frequencies and is inverted  $K$  times. The interference covariance matrix elements are computed by evaluating Equation (2.2) numerically, using Simpson's rule of numerical integration. For multiple interferers, the covariance matrix is evaluated using Equation (2.3). Adaptive array radiation patterns are computed by superimposing the quiescent radiation pattern with the weighted sum of auxiliary channel received voltages.

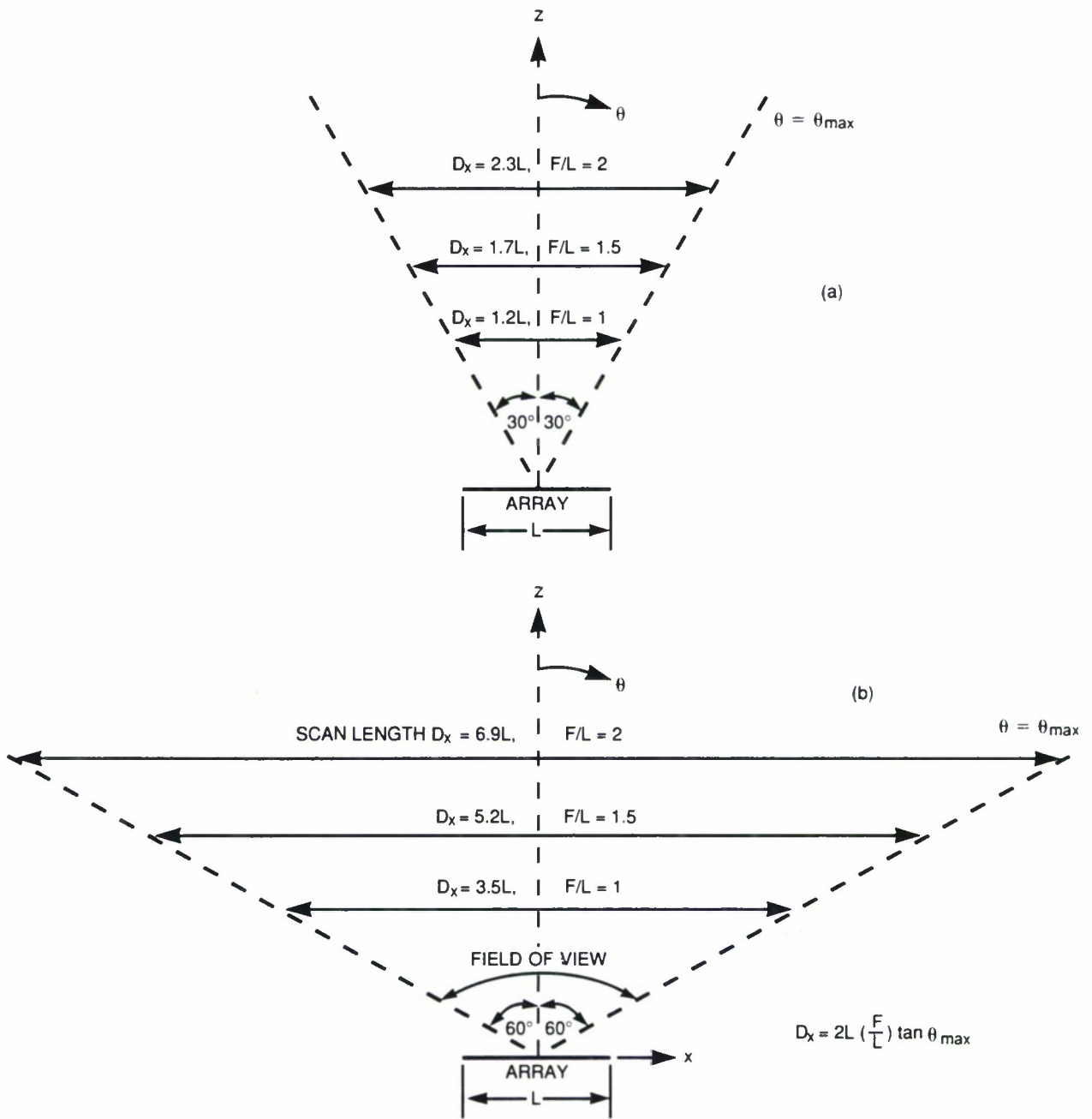


Figure 2-3. Example near-field scan lengths: (a) 60° and (b) 120° field of view.

### 3. RESULTS

#### 3.1 FOCUSED ARRAY QUIESCENT CONDITIONS

Consider a planar array of thin resonant monopoles having element length  $0.275 \lambda$  with wire radius  $0.007 \lambda$  and  $0.473 \lambda$  element spacing at center frequency 1.3 GHz. Such an array is useful for wide-angle scanning [16–18]. In standard spherical coordinates the principal polarization of a monopole array ( $z$ -directed elements) is the  $E_\theta$  component (or vertical polarization). The array is assumed to have 180 elements in a square lattice with 5 rows and 36 columns, and the array operates over an infinite ground plane as depicted in Figure 3-1. One current expansion function per array element is used, and so there are 180 unknowns in Equation (2.10). Assume that 32 of

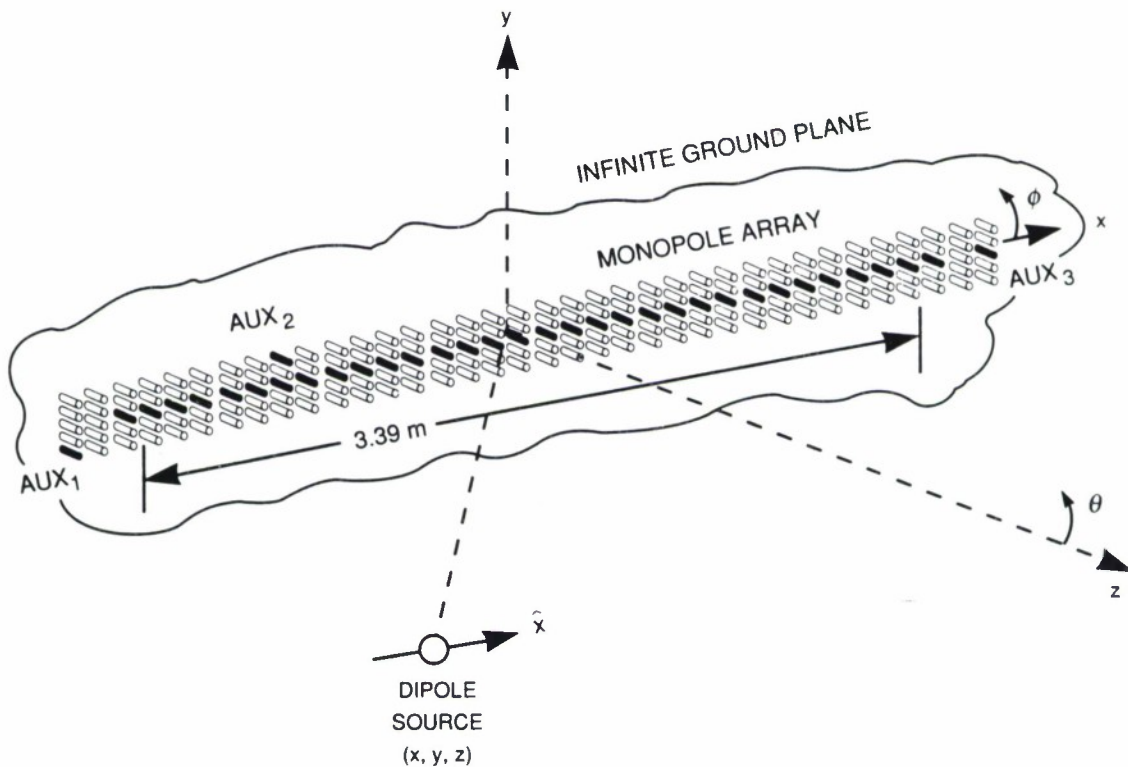


Figure 3-1. Planar array of monopoles with dipole source.

the elements in the center row are used to form the main channel output for a sidelobe canceller, that is,  $N_r = 32$ . The surrounding elements are effectively passively terminated (load impedance  $Z_L = 50 \Omega$  resistive) to guard the center elements from finite array edge effects. (Note: Auxiliary elements for the sidelobe canceller auxiliary channels will be selected from this guard band.) The active receive array length for this case is 11.11 ft (3.39 m). Referring to Figure 2-1, let  $z_F = F$  be the focal distance. Focal lengths of 1, 1.5, and 2  $L$  will be examined. The near-field desired field of view is assumed to be  $120^\circ$  as was shown in Figure 2-3(b). A scan angle of  $30^\circ$  from broadside and a Chebyshev illumination which generates  $-40$  dB uniform far-field sidelobes are assumed. A 40-ft near-field scan length was used at  $F/L = 1$  which provided a  $\pm 60^\circ$  field of view.

The monopole array near-field focused/near-field observation quiescent patterns are shown in Figure 3-2. Figure 3-2(a) shows the near-field result (dashed curve) obtained at  $F/L = 1$ . Included in this figure is the conventional far-field pattern (solid curve) observed at infinite range under the condition of focusing at infinite range. Figures 3-2(b) and (c) give the corresponding results at  $F/L = 1.5$  and  $F/L = 2$ , respectively. The half-power beam width is observed to be  $5.5^\circ$ . For  $F/L = 1$ , considerable degradation of the near-field main beam shape occurs below the half-power points. It can be noted that the near-field side-lobe envelope behaves much like that of the far-field side-lobe envelope, except in the vicinity of the main beam. Also, the near- and far-field nulls are not aligned. In particular, due to the finite range, the monopole element broadside null has filled in. As the near-field distance increases from  $L$  to  $2L$ , it is observed that the near-field pattern behaves more like that of the far-field pattern.

### 3.2 SIDE-LOBE CANCELLER ADAPTIVE ARRAY BEHAVIOR

In this section the adaptive nulling characteristics of a sidelobe canceller adaptive array are investigated. It is assumed that there are three auxiliary channels ( $N_{\text{aux}} = 3$ ), so the covariance matrix size is  $4 \times 4$  in this case, and there are four eigenvalues or degrees of freedom. The auxiliary element positions are designated by (row, column) and were chosen to be (1, 1), (5, 9), and (3, 36). Notice that the degrees of freedom have been allocated in two dimensions. The array quiescent conditions are the same as those described in Section 3.1. The quiescent radiation patterns were shown in Figure 3-2. Near-field ranges of  $F/L = 1, 1.5$ , and  $2$  are examined. In all near-field examples, the interference source range and focal range are equal. For the example array size, the actual near-field test distances are 3.39 m ( $F/L = 1$ ), 5.08 m ( $F/L = 1.5$ ), and 6.77 m ( $F/L = 2$ ). The far-field test distance is assumed to be at range  $F/L = \infty$ . A range of nulling bandwidths will be considered:  $B = 1$  MHz (narrowband,  $BL \cos \theta / c = 0.01$ ) to  $B = 100$  MHz (wideband,  $BL \cos \theta / c = 1$ ). Nonstressing and stressing interference scenarios will be examined. Nonstressing interference is defined as where the adaptive array degrees of freedom are sufficient to cancel the interference down to the noise level of the receiver. Stressing interference refers to the situation where the adaptive array degrees of freedom are insufficient for the adaptive output to reach the receiver noise floor.

#### 3.2.1 Nonstressing Interference: One Source

Consider the case of one interference source ( $J = 1$ ). Let an interferer, with power 50 dB above receiver noise at the array output, be located at  $\theta = 42^\circ$  both for finite and infinite range focused arrays. The covariance matrix elements defined in Equation (2.2) are evaluated using a 15-point Simpson's rule numerical integration.

For  $B = 1$  MHz, the adaptive array radiation patterns at center frequency 1.3 GHz are shown in Figure 3-3. Figure 3-3(a) is for a near-field distance of one aperture diameter ( $F/L = 1$ ). Figures 3-3(b) and (c) are for near-field ranges of  $1.5$  and  $2L$ , respectively. For each case, the adaptive cancellation ratio was computed to be 50 dB. The consumption of adaptive array degrees of freedom

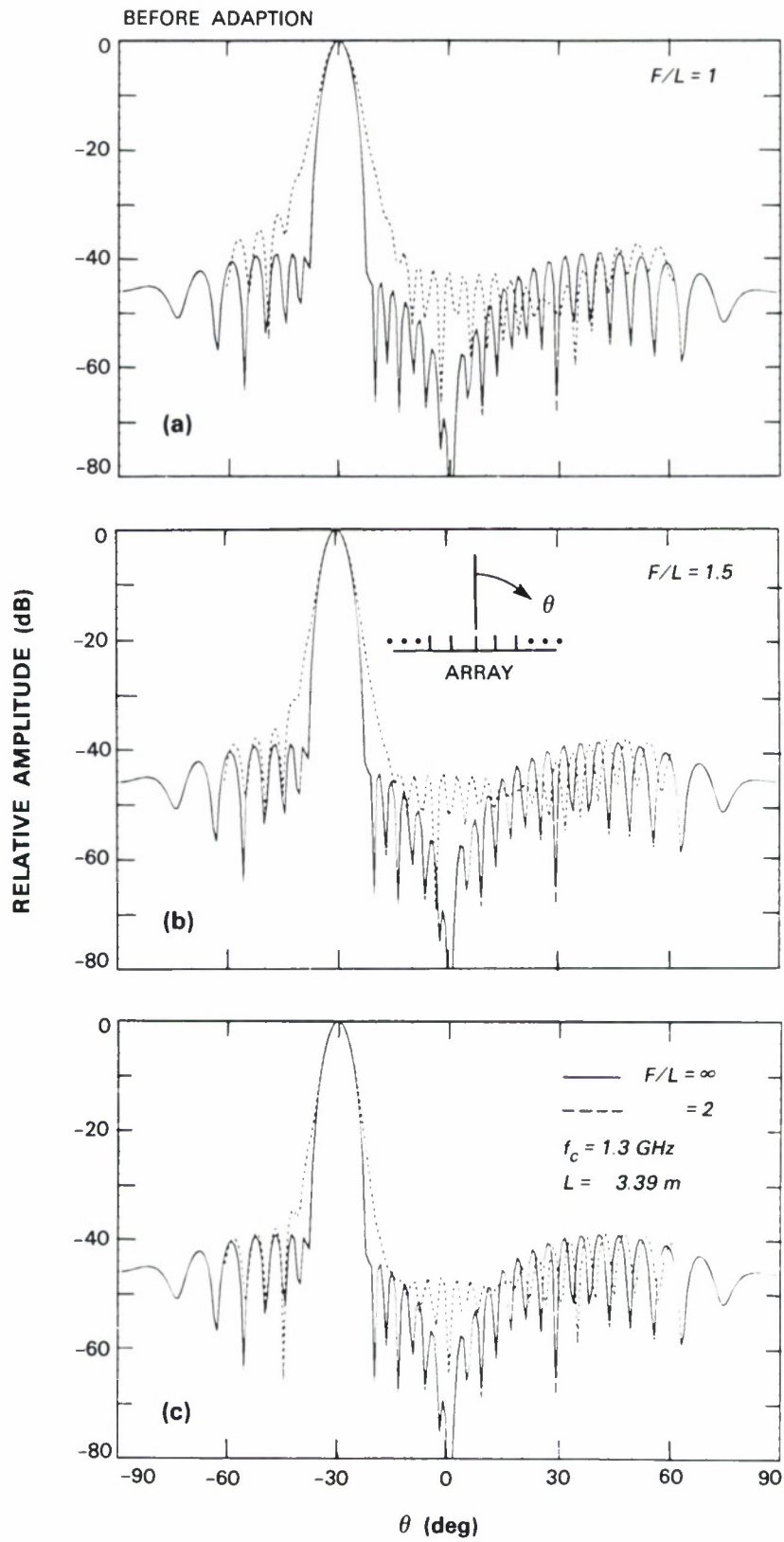


Figure 3-2. Monopole array NF/FF radiation patterns (one interferer) before nulling: (a)  $F/L = 1$ , (b)  $F/L = 1.5$ , and (c)  $F/L = 2$ .

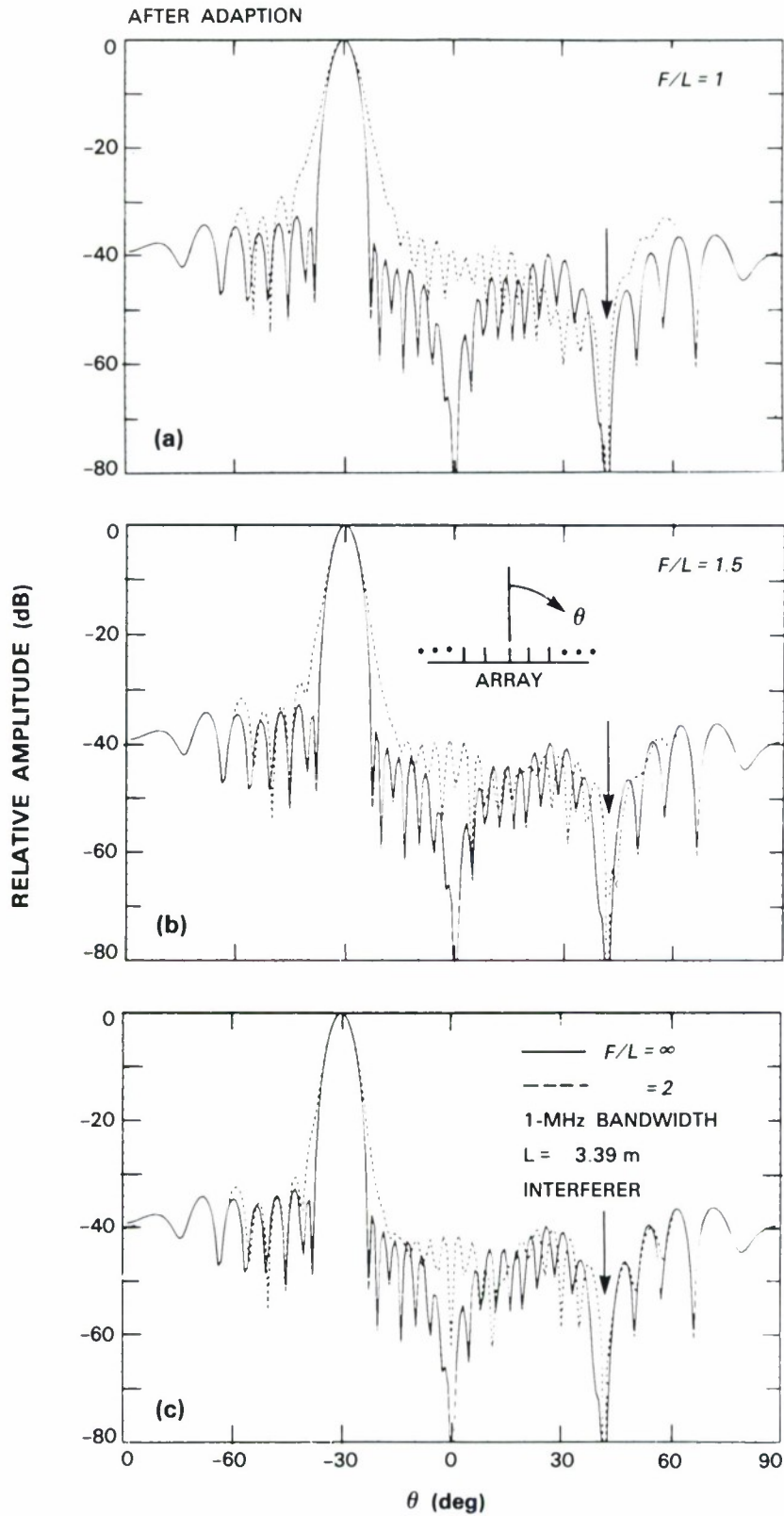


Figure 3-3. Monopole array NF/FF Radiation patterns after nulling: (a)  $F/L = 1$ , (b)  $F/L = 1.5$ , and (c)  $F/L = 2$ .

is depicted in Figure 3-4. It is seen that two eigenvalues are significantly above the receiver noise level. The remaining eigenvalues are at the receiver noise level (0 dB); thus, only two degrees of

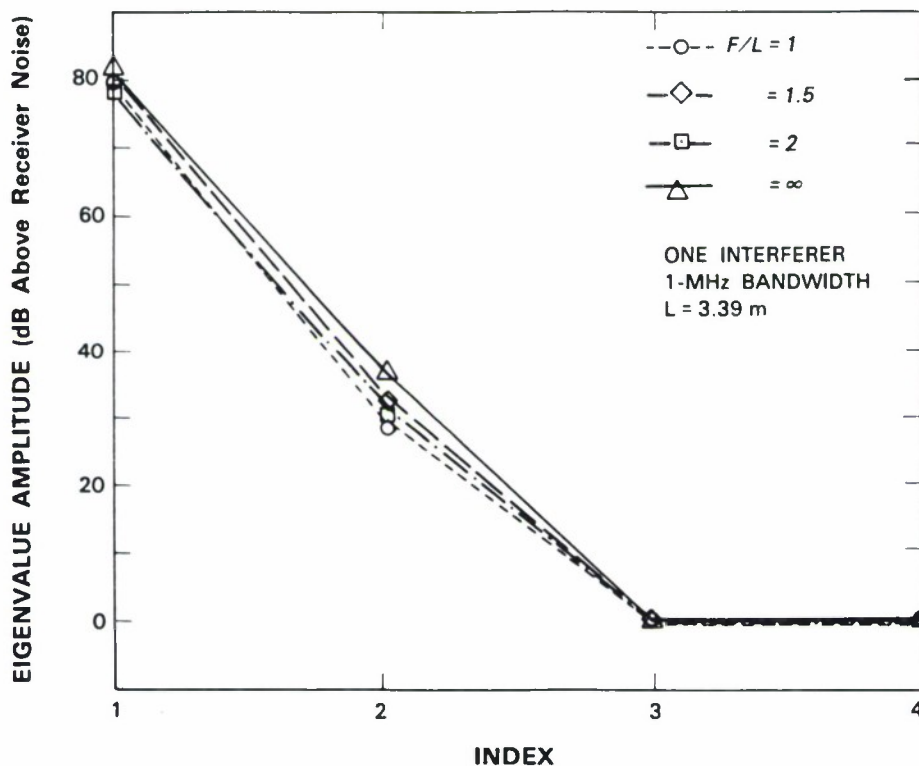


Figure 3-4. Covariance matrix eigenvalues for one NF/FF interferer.

freedom are engaged. The near-field eigenvalues are in good agreement with the corresponding far-field eigenvalues indicating that the degrees of freedom are consumed the same. The amplitude of the adaptive array NF/FF weights ( $w_a$ ) is given in Figure 3-5 and good agreement is evident. To show the behavior of a near-field null on the test plane, a two-dimensional contour radiation pattern has been computed for the  $F/L = 2$  case ( $z_F = 6.77$  m) and is given in Figure 3-6.

### 3.2.2 Stressing Interference: Two Sources

To demonstrate the validity of the NF/FF adaptive nulling equivalence for multiple sources, consider the previous array ( $N_r = 32$ ) and the present case with two interferers ( $J = 2$ ). Let the interferers be equal in power, uncorrelated, and located at  $\theta = 42^\circ, 47^\circ$ . (Note: The sources are

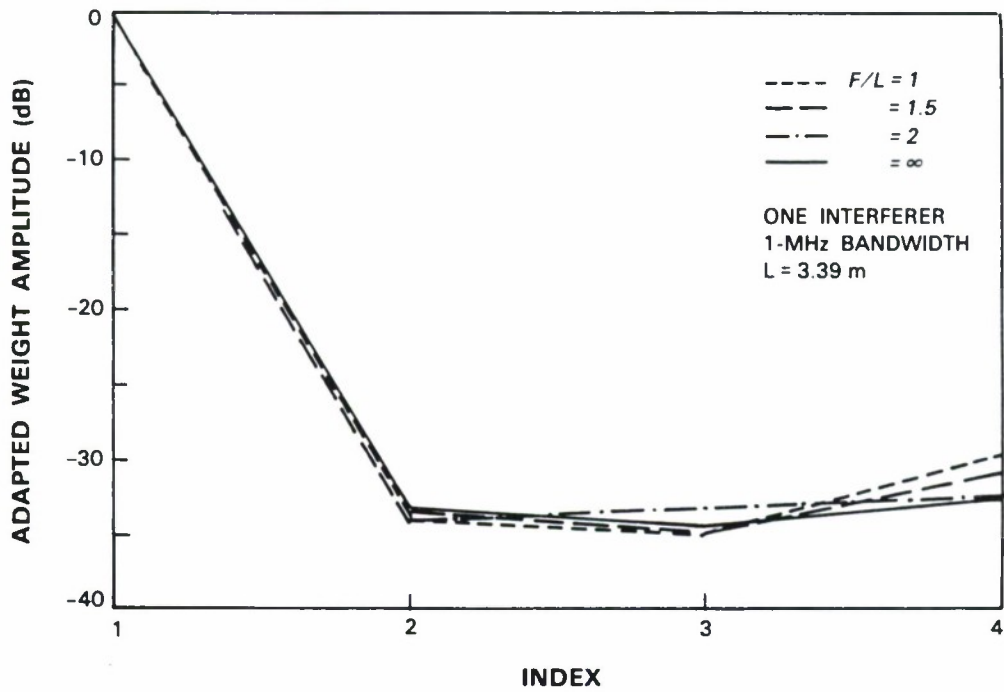


Figure 3-5. Amplitude of adaptive weights for one NF/FF interferer.

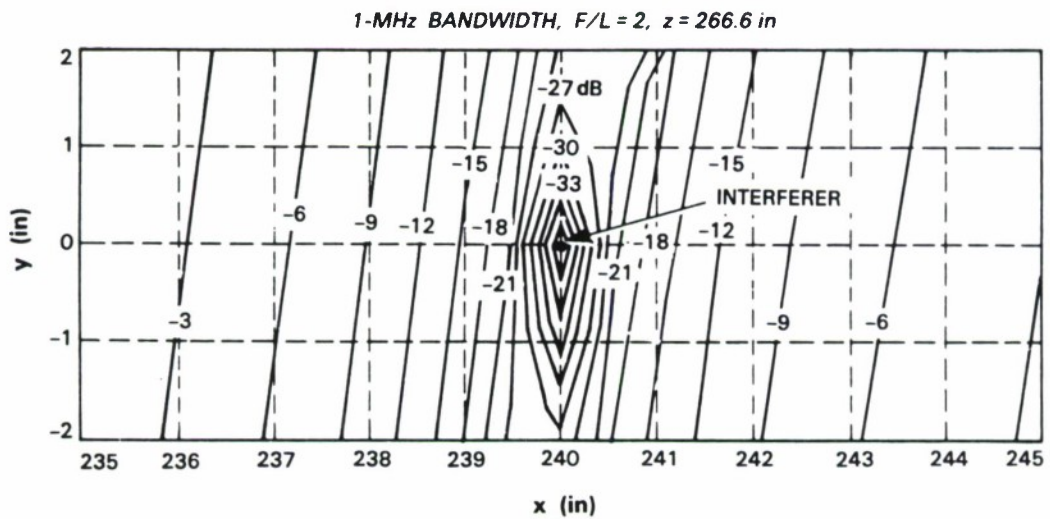


Figure 3-6. Two-dimensional near-field radiation pattern after adaption.

separated by approximately one half-power beamwidth.) The quiescent radiation patterns were shown in Figure 3-2. The total amount of interference power before adaption is set to 50 dB above noise at the array output.

For  $B = 1$  MHz, the NF/FF adaptive radiation patterns ( $F/L = 2$ ), at center frequency 1.3 GHz, are shown in Figure 3-7. It is observed that nulls are formed at the interferer positions. To compare near- and far-field consumption of the adaptive array degrees of freedom as a function of nulling bandwidth, the interference covariance matrix eigenvalues are presented in Figure 3-8 in the range ( $1 \leq F/L \leq 2$ ). Notice that each of the near- and far-field eigenvalues are in good agreement, that is,  $\lambda_1^{NF} \approx \lambda_1^{FF}$ ,  $\lambda_2^{NF} \approx \lambda_2^{FF}$ ,  $\dots$ ,  $\lambda_4^{NF} \approx \lambda_4^{FF}$ . Similarly, Figure 3-9 presents the adaptive cancellation as a function of nulling bandwidth. Complete cancellation,  $C = 50$  dB, is not achieved here for bandwidths greater than CW, because the interference is significantly stressing the adaptive array degrees of freedom. This is observed in Figure 3-8 which shows that for bandwidths greater than CW, all the covariance matrix eigenvalues are above receiver noise. At two aperture diameters source distance, the NF cancellation is equal to the FF cancellation over the entire bandwidth shown. The cancellation degrades by only about 3 dB, compared to the FF result, when the sources are at one aperture diameter distance. In this situation, the equivalence between near- and far-field sources is approximate. Finally, the adaptive array weights are shown in Figure 3-10 for the wideband case (100 MHz). Although there are some differences (in particular  $w_3$ ), the NF/FF weights are in good agreement.

From the above results, it is concluded that two near-field (or spherical wave) interferers, arranged equivalently in terms of angle, are equivalent to two far-field (or plane wave) interferers. A generalization of this statement would be that  $J$  near-field interferers are equivalent to  $J$  far-field interferers. This observation is consistent with the results presented in Reference 8.

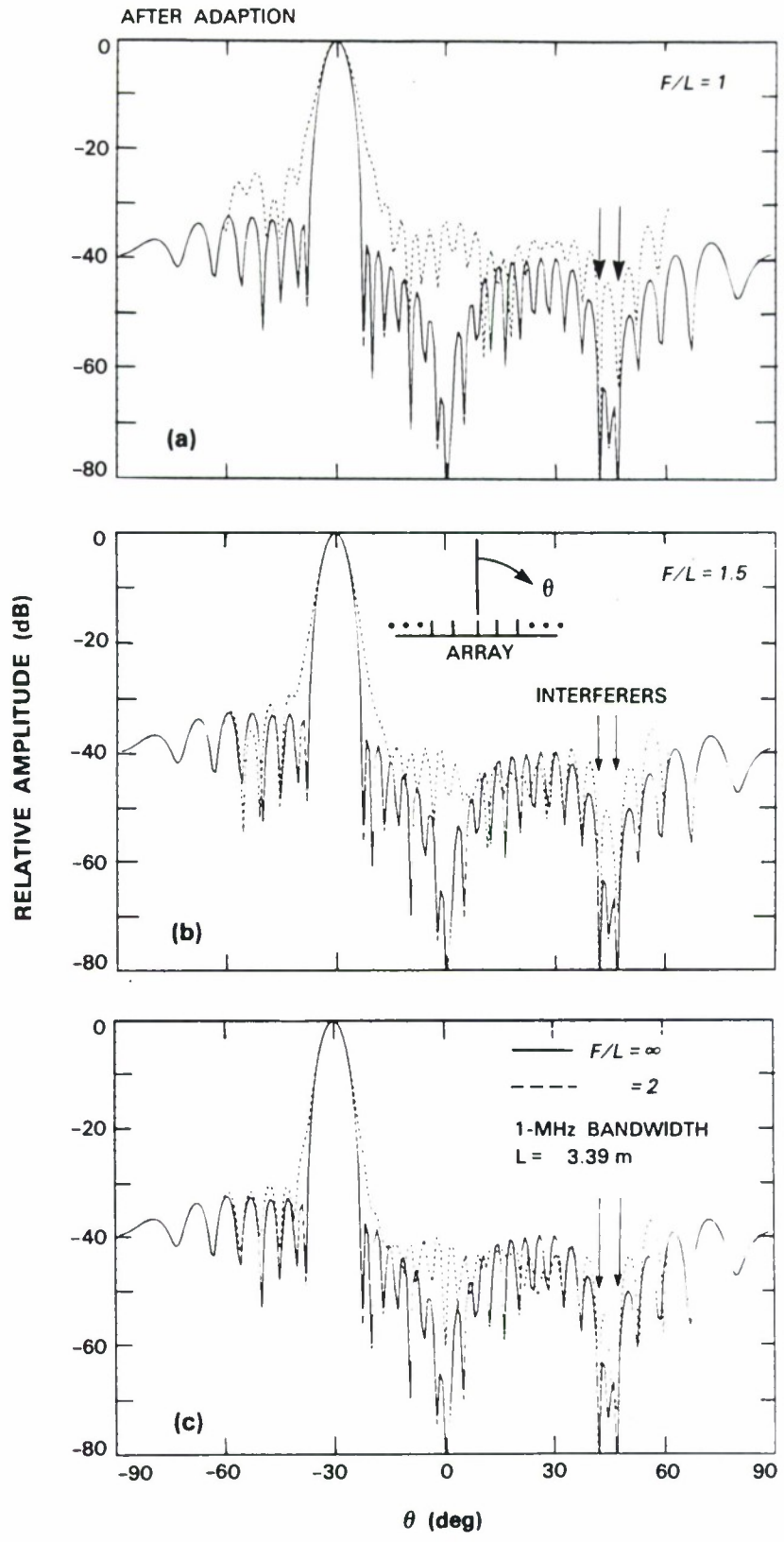


Figure 3-7. Monopole array NF/FF radiation patterns (two interferers) after nulling: (a)  $F/L = 1$ , (b)  $F/L = 1.5$ , and (c)  $F/L = 2$ .

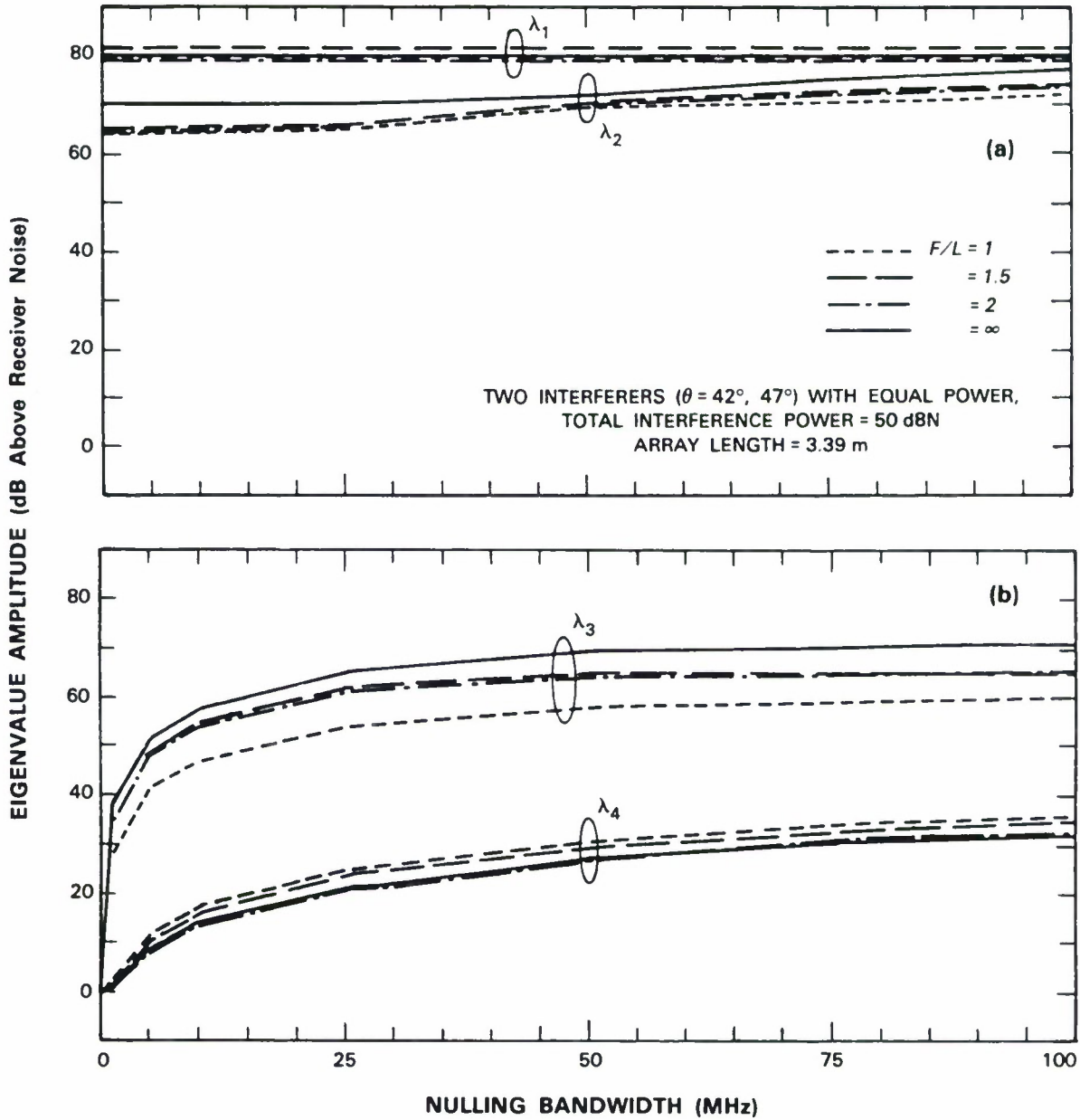
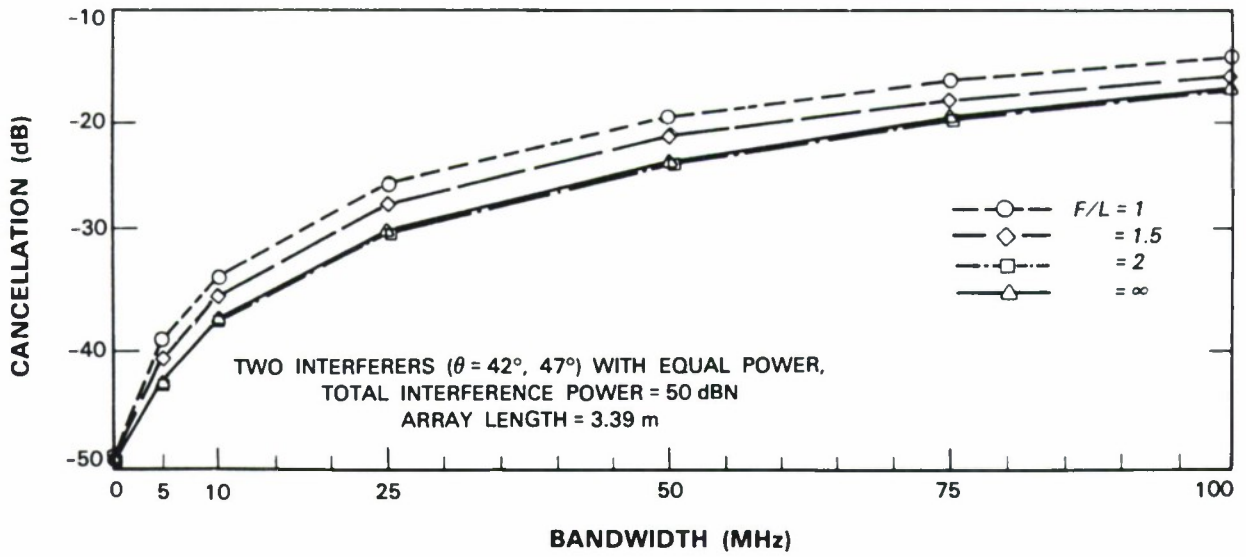
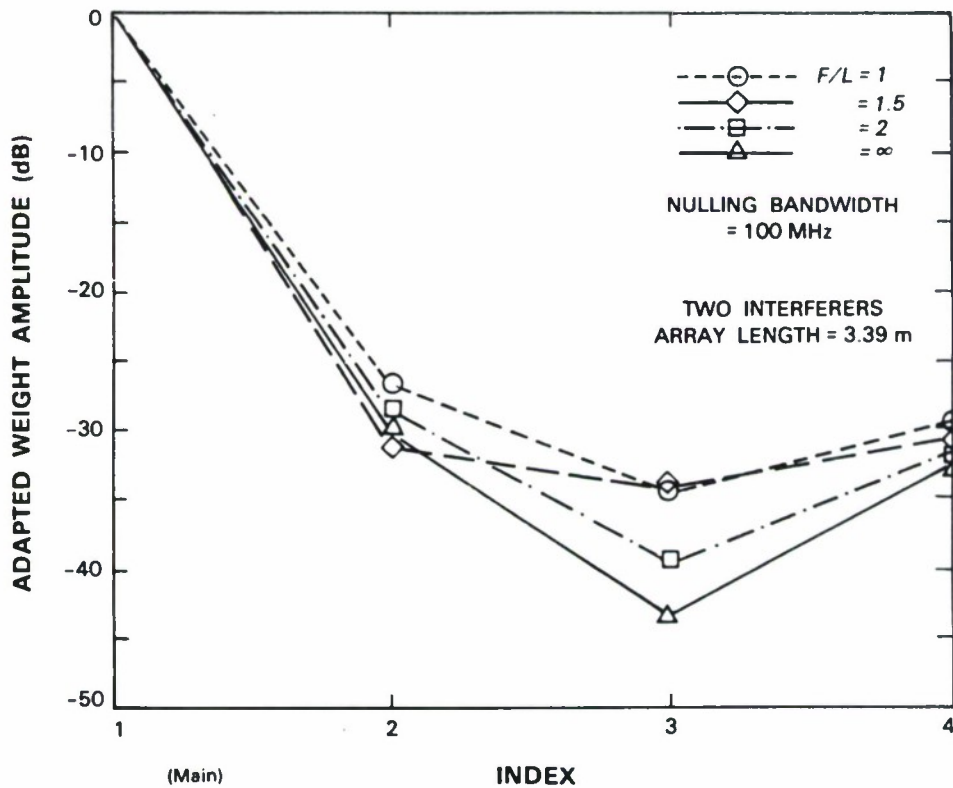


Figure 3-8. Covariance matrix eigenvalues for two NF/FF interferers versus nulling bandwidth: (a)  $\lambda_1, \lambda_2$  and (b)  $\lambda_3, \lambda_4$ .



115090-12

Figure 3-9. Adaptive cancellation for two NF/FF interferers versus nulling bandwidth.



115090-13

Figure 3-10. Amplitude of adaptive weights for two NF/FF interferers.

## 4. CONCLUSION

This report has discussed an approach to testing adaptive arrays in the near field. A theory for analyzing the behavior of an adaptive array, including bandwidth, polarization, and mutual coupling effects, in the presence of near-field interference has been developed. Near-field focusing has been used to establish effectively a far-field pattern in the near zone. The near-field range of interest here has been taken to be one to two aperture diameters of the antenna under test. Equations for calculating the adaptive array covariance matrix and antenna radiation patterns, for near-field (spherical wave) and far-field (plane wave) interference, were given. Numerical simulations of a partially adaptive planar array indicate that the radiation patterns, adapted weights, cancellation, and covariance matrix eigenvalues (degrees of freedom) are effectively the same for near- and far-field interference. Both nonstressing (single source) and stressing (multiple source) interference conditions have been analyzed. From the results shown, it can be inferred that  $J$  near-field interferers in the presence of a near-field focused adaptive array are equivalent to  $J$  far-field interferers in the presence of a far-field focused adaptive array. That is, a one-to-one correspondence can be made between near- and far-field interferers. Thus, a phased array antenna adaptive nulling system designed for far-field conditions can potentially be evaluated more conveniently using near-field interference sources. The adaptive antenna under test and interference sources can all be positioned within an anechoic chamber on the order of one to two times the antenna length. Experimental verification of this technique is desirable.

In this report, all sources (calibration and interference) were assumed to lie on a common test plane. This is not to restrict the technique but rather to have compatibility with planar near-field scanner hardware. The array had monopole elements and the interferer antenna was a one-half wavelength dipole. Not considered in this report are other, more conventional types of array antenna elements (broadside radiators) such as dipoles. These are to be addressed in a future report. Multiple phase centers, including mutual coupling effects with main beam clutter and sidelobe interference, will also be investigated in a future report.

## REFERENCES

1. A.D. Yaghjian, "An Overview of Near-Field Antenna Measurements," *IEEE Trans. Antennas Propag.* **AP-34**, 30 (1986).
2. R.C. Johnson, H.A. Ecker, and R.A. Moore, "Compact Range Techniques and Measurements," *IEEE Trans. Antennas Propag.* **AP-17**, 568 (1969).
3. J.T. Mayhan, "Some Techniques for Evaluating the Bandwidth Characteristics of Adaptive Nulling Systems," *IEEE Trans. Antennas Propag.* **AP-27**, 363 (1979).
4. W.F. Gabriel, "Adaptive Arrays – An Introduction," *Proc. IEEE* **Vol. 64**, 239 (1976).
5. A.J. Fenn, "A Near Field Technique for Phased Array Antenna Adaptive Nulling Performance Verification," Project Report SRT-24, MIT Lincoln Laboratory (November 1987).
6. A.J. Fenn, "Theory and Analysis of Near Field Adaptive Nulling," *IEEE Antennas Propag. Soc. 1986 Symp. Digest Vol. 2*, pp. 579-582.
7. A.J. Fenn, "Theory and Analysis of Near Field Adaptive Nulling," *1986 Asilomar Conf. on Signals, Systems, and Computers*, Washington, D.C.: Computer Society Press of the IEEE (1986), pp. 105-109.
8. A.J. Fenn, "Evaluation of Adaptive Phased Array Antenna Far Field Nulling Performance in the Near Field Region," Technical Report 822, MIT Lincoln Laboratory (1989).
9. A.J. Fenn, "Theoretical Near Field Clutter and Interference Cancellation for an Adaptive Phased Array Antenna," *IEEE Antennas Propag. Soc. 1987 Symp. Digest, Vol. 1*, pp. 46-59.
10. W.E. Scharfman and G. August, "Pattern Measurements of Phased-Arrayed Antennas by Focusing into the Near Zone," in *Phased Array Antennas, Proc. 1970 Phased Array Antenna Symp.*, A.A. Oliner and G.H. Knittel, eds., Dedham, Mass.: Artech House (1972), pp. 344-350.
11. R.A. Monzingo and T. W. Miller, *Introduction to Adaptive Arrays*, New York: Wiley (1980).
12. G. Strang, *Linear Algebra and Its Applications*, New York: Academic Press (1976).
13. W.L. Stutzman and G.A. Thiele, *Antenna Theory and Design*, New York: Wiley (1981).
14. I.J. Gupta and A.A. Ksienski, "Effect of Mutual Coupling on the Performance of Adaptive Arrays," *IEEE Trans. Antennas Propag.* **AP-31**, 785 (1983).
15. J.H. Richmond, "Radiation and Scattering by Thin-Wire Structures in a Homogeneous Conducting Medium (Computer Program Description)," *IEEE Trans. Antennas Propag.* **AP-23**, 412 (1975).
16. J.C. Herper and A. Hessel, "Performance of  $\lambda/4$  Monopole in a Phased Array," *IEEE Antennas Propag. Soc. 1975 Symp. Digest*, pp. 301-304.

17. A.J. Fenn, "Theoretical and Experimental Study of Monopole Phased Array Antennas," *IEEE Trans. Antennas Propag.* **AP-33**, 1118–1126 (1985).
18. H.M. Aumann and F.G. Willwerth, "Design and Performance of a Very Low Sidelobe Phased Array Antenna," Project Report SRT-31, MIT Lincoln Laboratory (1988).

## APPENDIX A

### DERIVATION OF ARRAY RECEIVED VOLTAGE MATRIX

The purpose of this appendix is to derive the expression for the array received voltage matrix which was given in Chapter 2, Equation (2.10):  $\mathbf{v}_j^{\text{rec}} = \mathbf{Z}_L [\mathbf{Z}^{\text{o.c.}} + \mathbf{Z}_L \mathbf{I}]^{-1} \mathbf{v}_j^{\text{o.c.}}$ . Consider Figure 2-2 which depicts the circuit model for a receive array and a source antenna. Let  $v_{n,j}^{\text{rec}}$  be the voltage received in the  $n$ th array element due to the  $j$ th source. The array elements are assumed to be terminated in a load impedance denoted  $Z_L$ , which in general is complex. The open-circuit mutual impedance between the  $m$ th and  $n$ th array elements is denoted by  $Z_{m,n}^{\text{o.c.}}$ . Similarly, the open-circuit mutual impedance between the  $n$ th array element and the  $j$ th source is denoted  $Z_{n,j}^{\text{o.c.}}$ . Now,  $i_{1,j}, i_{2,j}, \dots, i_{n,j}, \dots, i_{N,j}$  are the received terminal currents for the  $N$  array elements. The received voltages are related to the terminal currents and load impedances using

$$v_{n,j}^{\text{rec}} = -i_{n,j}^{\text{rec}} Z_L, \quad n = 1, 2, \dots, N. \quad (\text{A.1})$$

Let  $i_j$  be the terminal current of the  $j$ th source. The received voltages can be written as

$$\begin{aligned} v_{1,j}^{\text{rec}} &= i_{1,j}^{\text{rec}} Z_{1,1}^{\text{o.c.}} + i_{2,j}^{\text{rec}} Z_{1,2}^{\text{o.c.}} + \dots + i_{n,j}^{\text{rec}} Z_{1,n}^{\text{o.c.}} + \dots + i_{N,j}^{\text{rec}} Z_{1,N}^{\text{o.c.}} + i_j Z_{1,j}^{\text{o.c.}} \\ &\vdots \\ v_{n,j}^{\text{rec}} &= i_{1,j}^{\text{rec}} Z_{n,1}^{\text{o.c.}} + i_{2,j}^{\text{rec}} Z_{n,2}^{\text{o.c.}} + \dots + i_{n,j}^{\text{rec}} Z_{n,n}^{\text{o.c.}} + \dots + i_{N,j}^{\text{rec}} Z_{n,N}^{\text{o.c.}} + i_j Z_{n,j}^{\text{o.c.}} \\ &\vdots \\ v_{N,j}^{\text{rec}} &= i_{1,j}^{\text{rec}} Z_{N,1}^{\text{o.c.}} + i_{2,j}^{\text{rec}} Z_{N,2}^{\text{o.c.}} + \dots + i_{n,j}^{\text{rec}} Z_{N,n}^{\text{o.c.}} + \dots + i_{N,j}^{\text{rec}} Z_{N,N}^{\text{o.c.}} + i_j Z_{N,j}^{\text{o.c.}} \end{aligned} \quad (\text{A.2})$$

In the above equation, the term  $i_j Z_{n,j}^{\text{o.c.}}$  is the open-circuit voltage at the  $n$ th array element. Note: The index  $j$  for the  $j$ th source should not be confused with the indices used for the array elements.

Now, define

$$v_{n,j}^{\text{o.c.}} = i_j Z_{n,j}^{\text{o.c.}}, \quad (\text{A.3})$$

and using Equations (A.1) and (A.3) in Equation (A.2), rearrange the terms to yield

$$\begin{aligned} -v_{1,j}^{\text{o.c.}} &= i_{1,j}^{\text{rec}} (Z_{1,1}^{\text{o.c.}} + Z_L) + \dots + i_{n,j}^{\text{rec}} Z_{1,n}^{\text{o.c.}} + \dots + i_{N,j}^{\text{rec}} Z_{1,N}^{\text{o.c.}} \\ &\vdots \\ -v_{n,j}^{\text{o.c.}} &= i_{1,j}^{\text{rec}} Z_{n,1}^{\text{o.c.}} + \dots + i_{n,j}^{\text{rec}} (Z_{n,n}^{\text{o.c.}} + Z_L) + \dots + i_{N,j}^{\text{rec}} Z_{n,N}^{\text{o.c.}} \\ &\vdots \\ -v_{N,j}^{\text{o.c.}} &= i_{1,j}^{\text{rec}} Z_{N,1}^{\text{o.c.}} + \dots + i_{n,j}^{\text{rec}} Z_{N,n}^{\text{o.c.}} + \dots + i_{N,j}^{\text{rec}} (Z_{N,N}^{\text{o.c.}} + Z_L). \end{aligned} \quad (\text{A.4})$$

Equation (A.4) can be written in a more compact form as

$$-\mathbf{v}_j^{\text{o.c.}} = [\mathbf{Z}^{\text{o.c.}} + \mathbf{Z}_L \mathbf{I}] \mathbf{i}_j^{\text{rec}} \quad (\text{A.5})$$

where  $\mathbf{v}_j^{o.c.}$  is the open-circuit voltage matrix,  $\mathbf{Z}^{o.c.}$  is the open-circuit mutual impedance matrix,  $\mathbf{I}$  denotes the identity matrix, and  $\mathbf{i}_j^{rec}$  is the received terminal current matrix. From Equation (A.1) it is clear that

$$\mathbf{i}_j^{rec} = -\frac{\mathbf{v}_j^{rec}}{Z_L}. \quad (\text{A.6})$$

Substituting Equation (A.6) in (A.5) and solving for  $\mathbf{v}_j^{rec}$  yields

$$\mathbf{v}_j^{rec} = Z_L [\mathbf{Z}^{o.c.} + Z_L \mathbf{I}]^{-1} \mathbf{v}_j^{o.c.} \quad (\text{A.7})$$

which is the desired result.

## REPORT DOCUMENTATION PAGE

1a. REPORT SECURITY CLASSIFICATION Unclassified			1b. RESTRICTIVE MARKINGS			
2a. SECURITY CLASSIFICATION AUTHORITY			3. DISTRIBUTION/AVAILABILITY OF REPORT  Approved for public release; distribution is unlimited.			
2b. DECLASSIFICATION/DOWNGRADING SCHEDULE						
4. PERFORMING ORGANIZATION REPORT NUMBER(S)  Technical Report 842			5. MONITORING ORGANIZATION REPORT NUMBER(S)  ESD-TR-88-318			
6a. NAME OF PERFORMING ORGANIZATION  Lincoln Laboratory, MIT		6b. OFFICE SYMBOL <i>(If applicable)</i>		7a. NAME OF MONITORING ORGANIZATION  Electronic Systems Division		
6c. ADDRESS (City, State, and Zip Code)  P.O. Box 73 Lexington, MA 02173-0073			7b. ADDRESS (City, State, and Zip Code)  Hanscom AFB, MA 01731			
8a. NAME OF FUNDING/SPONSORING ORGANIZATION  HQ AF Space Division		8b. OFFICE SYMBOL <i>(If applicable)</i>  SD/XR		9. PROCUREMENT INSTRUMENT IDENTIFICATION NUMBER  F19628-85-C-0002		
8c. ADDRESS (City, State, and Zip Code)  Los Angeles AFB, CA 90009-2960			10. SOURCE OF FUNDING NUMBERS			
			PROGRAM ELEMENT NO.  63250F	PROJECT NO.  227	TASK NO.	WORK UNIT ACCESSION NO.
11. TITLE (Include Security Classification)  Moment Method Analysis of Near-Field Adaptive Nulling						
12. PERSONAL AUTHOR(S)  Alan J. Fenn						
13a. TYPE OF REPORT  Technical Report		13b. TIME COVERED FROM _____ TO _____		14. DATE OF REPORT (Year, Month, Day)  1989, April 7		15. PAGE COUNT  38
16. SUPPLEMENTARY NOTATION  None						
17. COSATI CODES			18. SUBJECT TERMS (Continue on reverse if necessary and identify by block number)			
FIELD	GROUP	SUB-GROUP				
			phased arrays	interference	near-field focusing	
			antennas	degrees of freedom	mutual coupling	
			adaptive nulling	near-field testing	method of moments	
			eigenvalues	far-field testing		
19. ABSTRACT (Continue on reverse if necessary and identify by block number)						
<p>A near-field technique which can be used to evaluate the far-field nulling characteristics of an adaptive phased array is investigated. The method of moments is used to analyze the performance of a side-lobe canceller adaptive phased-array antenna operating in the presence of near-field interference. Bandwidth, polarization, mutual coupling, and finite array edge effects are taken into account. Phased-array near-field focusing is used to produce an equivalent far-field antenna pattern at a range distance of one to two aperture diameters from the adaptive antenna under test. It is shown that the near-field adaptive nulling performance, with sources located on a test plane at one- to two-aperture-diameters range, is equivalent to conventional far-field adaptive nulling. The antenna analyzed is a planar array of monopole elements having multiple auxiliary channels. The interferer is assumed to be a band-limited noise source radiating from a dipole antenna. The adaptive nulling characteristics studied in detail are the array radiation patterns, adaptive cancellation, covariance matrix eigenvalues (degrees of freedom), and adaptive array weights.</p>						
20. DISTRIBUTION/AVAILABILITY OF ABSTRACT <input type="checkbox"/> UNCLASSIFIED/UNLIMITED <input checked="" type="checkbox"/> SAME AS RPT. <input type="checkbox"/> DTIC USERS				21. ABSTRACT SECURITY CLASSIFICATION  Unclassified		
22a. NAME OF RESPONSIBLE INDIVIDUAL  Lt. Col. Hugh L. Southall, USAF			22b. TELEPHONE (Include Area Code)  (617) 981-2330		22c. OFFICE SYMBOL  ESD/TML	